Macrocellular titanosilicate monoliths as highly efficient structured olefin epoxidation catalysts

Valentin Smeets,[a] Ludivine van den Biggelaar,[a] Tarek Barakat,[b] Eric M. Gaigneaux,[a] and Damien P. Debecker*[a]

Abstract: Self-standing macrocellular titanosilicate monolith foams are obtained using a one-pot sol-gel route and show excellent performance in the epoxidation of cyclohexene. Thanks to the High Internal Phase Emulsion (HIPE) templating method, the materials feature a high void fraction, a hierarchically porous texture and good mechanical strength. Highly dispersed Ti species can be incorporated in tetrahedral coordination the silica matrix. These characteristics allow the obtained 'SiTi(HIPE)' materials to reach high catalytic turnover in the epoxidation of cyclohexene. The monoliths can advantageously be used to run the reaction in continuous flow mode.

Titanosilicates are an important class of materials that catalyze selective oxidation reactions.[1] For example, the combination of TS-1 zeolite – in which Ti atoms substitute Si atoms in the crystalline framework – with H_2O_2 is omnipresent in industrial applications, notably for hydroxylation and epoxidation reactions.[2,3] The crystallinity and the intrinsic hydrophobicity of TS-1 make this material particularly efficient to catalyze the oxidation of small substrates with high selectivities.[4]

However, the microporosity of TS-1 makes it less efficient for the conversion of bulky olefins, as the restricted diffusion of the reactants and products in and out the porosity can severely lower the catalytic activity which is consequently mainly restrained to the external surface.[5,6] An additional limitation is linked with the fact that the Ti loading incorporated into the zeolitic framework can hardly be tuned – with a typical maximal Ti loading of 2.5 % (here and after the loading is expressed as mol Ti / (mol Ti + mol Si) × 100 %).[7] These issues triggered intensive research on the incorporation of titanium in silica-based materials with larger pores in order to broaden the range of applications for titanosilicates.[8–10] New strategies in this field are still flourishing, taking benefits of innovative sol-gel routes[11] involving templating methods – possibly combined to supercritical[12,13] or aerosol[14,15] drying strategies – or realized under non-aqueous conditions.[16–18]

Despite those successes, the resulting materials are often obtained in the form of fine powders which require further steps to shape the catalyst as extrudates, pellets or monoliths, before they could be used in industrial flow processes.[19] This step represents an additional challenge as it necessitates a fine control of the mechanical properties and the diffusion regimes without sacrificing the intrinsic performance of the catalyst. Alternatively, the catalyst can be dispersed onto a pre-shaped solid support[20–22] that should meet several specifications (texture, surface composition, mechanical stability, etc.). With such strategy, a challenge is to maximize the loading and the dispersion of the catalyst while avoiding leaching and/or deactivation.[23] Thus, the one-step preparation of Ti-containing materials that do not require further shaping steps is highly sought for.[24,25]

The "High Internal Phase Emulsion" (HIPE) method (Figure 1) has been described in the literature for the preparation of monolithic foams of silica 'Si(HIPE)',[26] and more recently acidic aluminosilicates 'SiAl(HIPE)'.[19] Mixed oxides silica/titania 'SiO_2/TiO_2(HIPE)' monoliths – with TiO_2 domains grown in the silica framework – were also developed for optical application.[27] The shape and the high void fraction of these macrocellular foams make them particularly suitable to be used in continuous flow reactors.[28] Also, the specific surface area – which is generally high due to the presence of micro- and mesopores in the macropore walls – can be easily functionalized, allowing the monolith to be used as support for catalyst particles and enzymes.[29–32]

Apart from the materials texture, structure and morphology, the Ti speciation is also a crucial parameter. The high dispersion of Ti inside the silica network is a prerequisite for the targeted application, since isolated titanium atoms in tetrahedral coordination are identified as the active sites for olefin epoxidation.[3,4] Such quest for homogeneity in mixed oxide catalysts is a perpetual challenge for sol-gel chemistry because different precursors tend to exhibit different reactivity.[33]

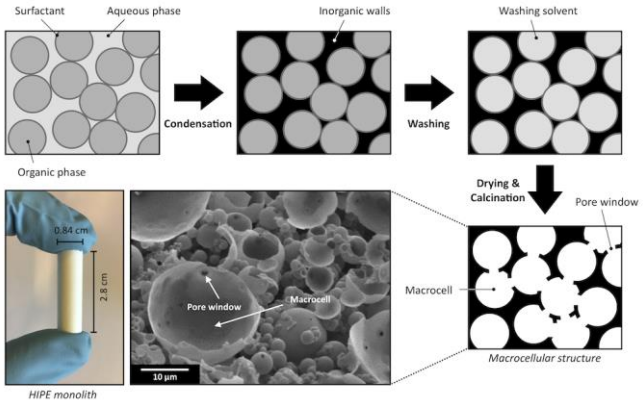


Figure 1. Schematized mechanism for the formation of HIPE monolith foam. An actual picture of the **SiTi(HIPE)_5%** monolith (left) and a SEM micrograph of a scratched piece of **SiTi(HIPE)_5%** (right) are shown for comparison. Additional SEM micrographs can be found in the Supporting Information (Figure S1).

[a] *V. Smeets, Dr. L. van den Biggelaar, Prof. E.M. Gaigneaux, Prof. D.P. Debecker*
Institute of Condensed Matter and Nanosciences (IMCN)
UCLouvain
Place Louis Pasteur, 1, Box L4.01.09, 1348 Louvain-la-Neuve, Belgium
E-mail: Damien.debecker@uclouvain.be
[b] *Dr. T. Barakat*
Laboratory of Inorganic Materials Chemistry
UNamur
Rue de Bruxelles, 61, 5000 Namur, Belgium

Supporting information for this article is given via a link at the end of the document.

Table 1. Textural properties (measured by mercury porosimetry intrusion and N_2 physisorption) and compressive strength of the monoliths.

	Intrusion volume ($cm^3.g^{-1}$)	Porosity (%)	Bulk density ($g.cm^{-3}$)	Skeletal density ($g.cm^{-3}$)	S_{BET} ($m^2.g^{-1}$)	S_μ ($m^2.g^{-1}$)[a]	V_p ($cm^3.g^{-1}$)[b]	V_μ ($cm^3.g^{-1}$)[a]	R_S (MPa)[c]
TS-1	–	–	–	–	510	380	0.43	0.15	–
Si(HIPE)	10.3	85	0.083	0.57	700	200	0.33	0.08	0.42
SiTi(HIPE)_1.8%	11.5	87	0.076	0.60	1000	460	0.46	0.18	0.52
SiTi(HIPE)_5%	10.5	87	0.083	0.62	950	470	0.43	0.19	0.45
SiTi(HIPE)_10%	4.8	84	0.177	1.12	1010	370	0.52	0.15	0.81

[a] Micropore specific surface area and volume calculated from the t-plot. [b] Measured at $P/P_0 = 0.98$. [c] R_S expresses the crush strength of the monoliths.

To the best of our knowledge, there is no report on the fabrication of Ti-containing Si(HIPE), that could be coined 'SiTi(HIPE)' to account for the fact that Ti is dispersed in the silica material. Thus, in this study, we propose to adapt the emulsion-based acidic sol–gel route used for the preparation of Si(HIPE) monoliths[26] in order to incorporate highly dispersed titanium species. By doing so, we aim to obtain – in one-step – catalytically active self-standing monoliths that can also be used to run epoxidation reactions in continuous flow mode.

The full protocol is described in the Supporting Information. Briefly, a precise amount of titanium isopropoxide is added in an acidic aqueous phase – containing tetradecyltrimethylammonium bromide (TTAB) – which is kept under vigorous stirring for 1h before the addition of tetraethyl orthosilicate (TEOS). Dodecane is then added under stirring to form a stable emulsion that is poured in a cylindrical vial and allowed to age for one week at room temperature. After washing, drying, and calcination, we obtained cylindrical self-standing monoliths of centimeter dimensions (Figure 1). The catalysts were denoted **'SiTi(HIPE)_X%'**, where "X" stands for the nominal Ti loading. The nominal loading was investigated in the 1.8–10 % range. **Si(HIPE)** monolith, without titanium, was also prepared for comparison.[29]

Macroscopically, we observed a shrinkage of the **Si(HIPE)** monolith diameter as compared to the size of the wet gel formed in the vial (*ca.* 28%). This shrinkage tends to be more important upon incorporation of titanium in the material: 34 and 35 % with 1.8 and 5 % Ti, respectively (see Figure S2 in the Supporting Information). However, the shrinkage was more pronounced for the monolith loaded with 10% Ti (52 % relative shrinkage). This coincides with higher bulk and skeletal densities – deduced from mercury intrusion porosimetry data – as well higher as compressive strength (Table 1). A similar trend was previously reported for SiO_2/TiO_2(HIPE).[27]

After crushing the monoliths, the samples were analyzed by SEM (Figure 1**).** TiSi(HIPE) samples showed a macrocellular structure with cells of *ca.* 1–40 µm. No visible difference could be observed when varying the amount of titanium. Compared to the well-described silica HIPE,[34] the macro-cells of SiTi(HIPE) monoliths are smaller. Since Ti^{4+} can act as a Lewis acid catalyst,[33] we assume that condensation reactions occur faster during the synthesis of SiTi(HIPE), generating high shearing forces earlier in the emulsion process and thus reducing the oil droplet diameters.[19] This is consistent with the shrinkage observed at the macroscopic scale when Ti is incorporated.

The size of the macroscopic pore windows was evaluated by mercury intrusion measurements (Figure S3). The pore size distributions reveal a bimodal porosity in all samples, one in the 10–100 nm region, the other spreading between 1 and 10 µm. Generally speaking, incorporating titanium in the monolith framework leads to a decrease in size for the latter contribution. In **Si(HIPE)**, the distribution is centered around 5 µm, whereas it is centered at *ca.* 1–2 µm for SiTi(HIPE). Among the SiTi(HIPE) series, **SiTi(HIPE)_10%** shows the highest decrease of the pore window, as well as the lowest intrusion volume (Table 1). Below 10% of Ti, the intrusion volume was not modified compared to **Si(HIPE)**.

Table 2. Percentage of Ti species (mol Ti / (mol Ti + mol Si) × 100 %) in the catalysts (bulk composition, ICP-AES) and at the catalyst surface (from XPS).

	Bulk Ti %[a]	Surf. Ti %	Surf. Ti–O–Si %	% Ti–O–Si[b]
TS-1	1.6 (1.8)	1.3	1.2	90
SiTi(HIPE)_1.8%	0.6 (1.8)	0.4	0.4	100
SiTi(HIPE)_5%	1.5 (5.0)	1.2	1.0	83
SiTi(HIPE)_10%	2.9 (10.0)	2.3	1.9	83

[a] Nominal composition is given in brackets. [b] % Ti–O–Si = (Surf. Ti–O–Si % / Surf. Ti %) × 100.

The elemental analysis of the monoliths showed that the experimental Ti mol.% was lower than the nominal one, with only *ca.* 30% of the introduced titanium incorporated in the silica framework (Table 2). The remaining Ti was presumably lost during the washing steps. Nevertheless, the amount of incorporated Ti is proportional to the nominal loading (Figure S4). For comparison, we prepared a titanosilicalite-1 (**TS-1**) zeolite catalyst with a nominal Ti loading of 1.8 %.[35]

In all tested catalysts, the surface seems to be slightly enriched with Si, as the Ti surface composition – determined by XPS on basis of the Ti 2p peak – is lower than the bulk composition. The deconvolution of the Ti 2p peak of the catalysts (Figure S5) allows to distinguish the fraction that is truly incorporated into the silica matrix ("% Ti–O–Si" in Table 2) from the fraction that is not dispersed and instead present as TiO_2 inclusions. The former is found at 460.00 eV and the latter is found at 458.5 eV.[36,37] Interestingly, more than 80% of the titanium at the SiTi(HIPE) catalysts surface is in the highly dispersed form. This value is in the same range as the value measured for **TS-1**, which is known to incorporate almost all the Ti atoms in its well defined crystalline framework.

To go deeper in the investigation of the Ti coordination, the band gap energy (E_g) of the SiTi(HIPE) catalysts was calculated from the optical absorption edges in the DR UV-vis spectra of the materials. The results indicate that the E_g value decreases with higher amount of Ti: 5.63, 5.48 and 5.32 eV for **SiTi(HIPE)_1.8%**, **SiTi(HIPE)_5%** and **SiTi(HIPE)_10%**, respectively (Figure S6). For titanosilicates, it was previously reported that a higher E_g value is related to a relatively higher amount of isolated tetrahedral Ti^{4+} species.[38] As we observed a decrease of the E_g value at higher Ti loadings, we can assume that increasing the amount of titanium leads to a lower proportion of tetrahedral Ti species.

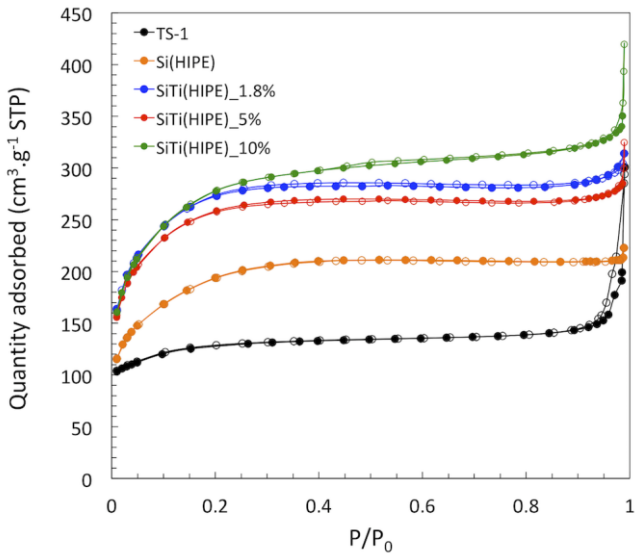


Figure 2. Nitrogen physisorption isotherms of the HIPE catalysts compared to **TS-1**.

Nitrogen physisorption measurements (Figure 2) revealed that the SiTi(HIPE) catalysts all have similar BET area in the 950–1010 $m^2.g^{-1}$ range (Table 1). This is higher than the value found experimentally for **Si(HIPE)** of 700 $m^2.g^{-1}$. This is presumably ascribed to a higher proportion of micropores in the SiTi(HIPE) catalysts. Indeed, according to the t-plot, the micropore surface area is between 370 and 470 $m^2.g^{-1}$ for SiTi(HIPE) catalysts, which is higher than the value of 200 $m^2.g^{-1}$ obtained for **Si(HIPE)**, suggesting an influence of the incorporation of titanium on the formation of micropores. From the BJH pore size distribution at adsorption (data not shown), mesopores above 3 nm do not contribute significantly to the surface area. This therefore suggests the presence of small mesopores, which are more present in **SiTi(HIPE)_10%**, as evidenced by the forced closure of the isotherm at P/P_0 of 0.4–0.5. As a comparison, **TS-1** catalyst displays a BET surface area of 510 $m^2.g^{-1}$ with an estimated micropore area of 380 $m^2.g^{-1}$.

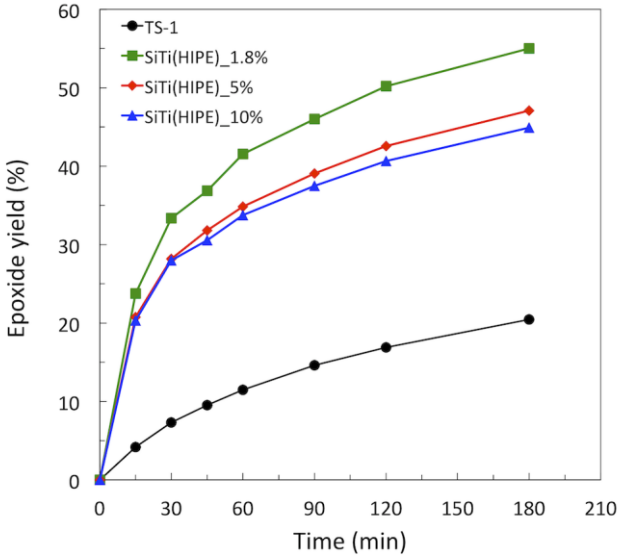


Figure 3. Epoxidation yield for the Ti-catalyzed conversion of cyclohexene into cyclohexene oxide in toluene using cumene hydroperoxide (CHP) as oxidant. Experimental conditions: T = 90°C, [CATA] = 5 $g.l^{-1}$, [Cyclohexene] = 0.9 $mol.l^{-1}$, [CHP] = 0.18 $mol.l^{-1}$.

The catalytic performance was first investigated in batch mode by grinding the monoliths into fine powder. As a first assessment of the catalytic performance, we tested the activity of **SiTi(HIPE)_5%** in the epoxidation of cyclohexene in acetonitrile using hydrogen peroxide (30% w/w aqueous solution) as oxidant and we compared it to **TS-1**. The macrocellular catalyst was approximately two times more active than the microporous reference while maintaining a high selectivity (see experimental details in the supplementary information and Figure S7). An even more efficient epoxidation reaction can be designed using cumene hydroperoxide (CHP) as the oxidant and toluene as the solvent.[39] Thus, we have tested our macrocellular Ti-based catalysts in this model reaction. Results presented in Figure 3 show a much higher epoxide yield for all SiTi(HIPE) catalysts

compared to **TS-1**, with selectivity for cyclohexene oxide in the 81–97% range (complete data set can be found in Table S1). Since **SiTi(HIPE)_5%** and **TS-1** were shown to have similar tetrahedral Ti contents by XPS, the higher activity of **SiTi(HIPE)_5%** is a clear evidence of the role of the textural properties on the catalytic performance. Indeed, the high surface area of the SiTi(HIPE) catalysts – even excluding micropores – suggests that these materials are good candidates as catalysts for the conversion of bulky olefins such as cyclohexene. On the contrary, TS-1 zeolite is mainly microporous, with channels having dimensions of *ca.* 5 Å[40] that prevent cyclohexene and CHP from entering the pores. The accessible surface area of SiTi(HIPE) is therefore about four times higher than **TS-1**, with benefit for the conversion of cyclohexene. Consistently, the initial turnover frequency (TOF), approximated by the CHP conversion at the early stage of the reaction (15 min) is 192 h^{-1} for **SiTi(HIPE)_5%**, and only 38 h^{-1} for **TS-1** (Table S1).

Among the series of SiTi(HIPE) catalysts, we see that increasing the amount of Ti decreases the activity, with a clear correlation with the measured E_g values and thus with the Ti coordination mode (Figure 4).[15,38] When the amount of Ti is increased, the formation of octahedral species is favored, which lowers the specific activity.

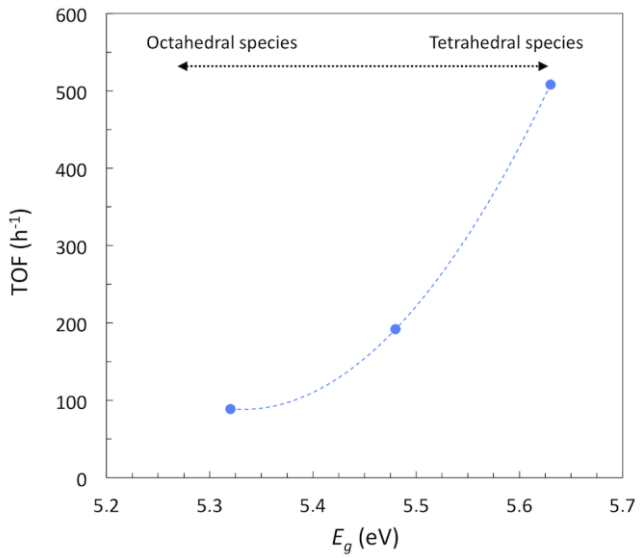


Figure 4. Correlation between the E_g value of the tested catalysts and the corresponding TOF value for the conversion of cyclohexene into cyclohexene oxide.[38]

To validate our synthetic approach in the perspective of process intensification, a monolith was tested in continuous flow mode for the conversion of cyclohexene with CHP (Figure 5). To do so, the self-standing monolith was casted in an inert heat-shrinkable polytetrafluoroethylene (PTFE) membrane and connected to a syringe-pump able to deliver a precise and tunable flow rate (see inset of Figure 5 and Supporting Information for the detailed procedure).[29] The epoxide yield was dependent on the contact time (complete data can be found in Figure S8 and Table S2 of the Supporting Information). For example, at 15 min contact time, the epoxide yield reaches 20%, exactly like in the batch mode. The selectivity for cyclohexene oxide was always between 74 and 98%, which is similar to values obtained in batch reactor.

In conclusion, we showed that combining silicon and titanium precursors in the synthesis of SiTi(HIPE) monolith foams allowed the formation of a functional material presenting similar mechanical and textural properties compared to the parent Si(HIPE) monolith, while ensuring a high dispersion of the titanium species in tetrahedral coordination state. This contributes to the much higher intrinsic activity of these materials compared to the reference TS-1 catalyst. When the Ti loading remained low (around 1 mol.%) the formation of oligomeric titanium species was avoided and the specific catalytic activity was outstanding. The results obtained for the conversion of cyclohexene with CHP in continuous flow mode make these materials attractive for the production of epoxides in continuous flow processes.

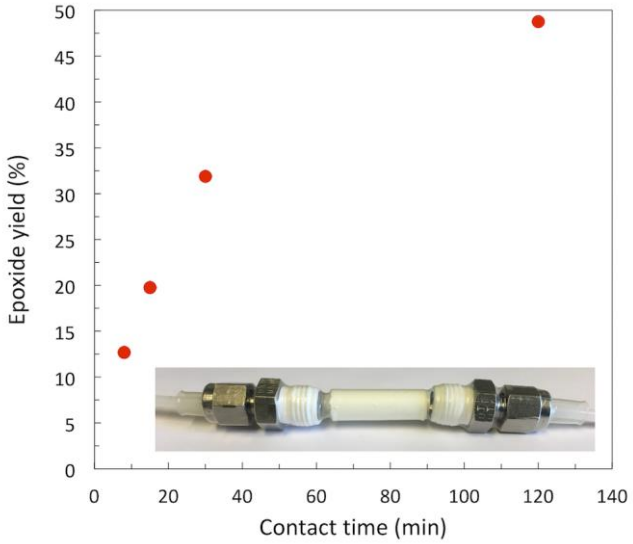


Figure 5. Epoxidation yield-contact time dependence in the Ti-catalyzed conversion of cyclohexene with CHP using **SiTi(HIPE)_5%** in continuous flow mode. In inset is shown a picture of the continuous flow reactor showing the **SiTi(HIPE)_5%** monolith casted in the heat-shrinkable PTFE membrane. Experimental conditions: T = 90°C, 100 mg CATA, [Cyclohexene] = 0.9 $mol.l^{-1}$, [CHP] = 0.18 $mol.l^{-1}$. Complete data set available in Figure S8.

Experimental Section

Experimental details are provided as supplementary information.

Acknowledgements

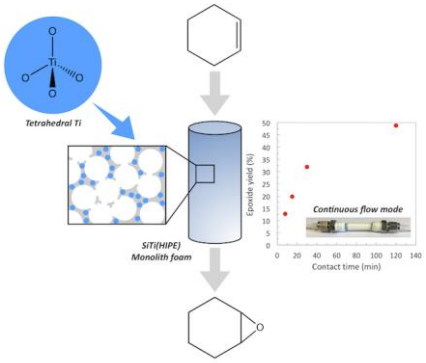
Authors acknowledge the 'Communauté française de Belgique' for the financial support through the ARC programme (15/20-069). F. Devred and J. Vanderclausen are acknowledged for the technical and logistical support. V. Smeets is thankful to F.R.S.–F.N.R.S. for his FRIA PhD grant. F.R.S.–F.N.R.S. is also thanked

for the acquisition of the UV-Vis equipment used here (project CDR J.0156.18, supervisor E.M. Gaigneaux).

Keywords: High Internal Phase Emulsion • monolith foam • titanosilicate • cyclohexene epoxidation • continuous flow

[1] M. Taramasso, G. Perego, B. Notari, *Preparation of Porous Crystalline Synthetic Material Comprised of Silicon and Titanium Oxides*, **1983**, US4410501A.
[2] C. Perego, A. Carati, P. Ingallina, M. A. Mantegazza, G. Bellussi, *Appl. Catal. A: General* **2001**, *221*, 63–72.
[3] M. G. Clerici, P. Ingallina, *J. Catal.* **1993**, *140*, 71–83.
[4] M. G. Clerici, *Kinet. Catal.* **2015**, *56*, 450–455.
[5] R. Murugavel, H. W. Roesky, *Angew. Chem. Int. Ed.* **1997**, *36*, 477–479.
[6] M. Hartmann, A. G. Machoke, W. Schwieger, *Chem. Soc. Rev.* **2016**, *45*, 3313–3330.
[7] R. Millini, E. Previde Massara, G. Perego, G. Bellussi, *J. Catal.* **1992**, *137*, 497–503.
[8] A. Corma, *Chem. Rev.* **1997**, *97*, 2373–2419.
[9] T. Blasco, A. Corma, M. T. Navarro, J. P. Pariente, *J. Catal.* **1995**, *156*, 65–74.
[10] M. A. Camblor, A. Corma, A. Martínez, J. Pérez-Pariente, *J. Chem. Soc., Chem. Commun.* **1992**, *0*, 589–590.
[11] D. P. Debecker, *Chem. Rec.* **2018**, 18, 662-675.
[12] R. Hutter, T. Mallat, D. Dutoit, A. Baiker, *Topics Catal.* **1996**, *3*, 421–436.
[13] G. M. Pajonk, *Appl. Catal.* **1991**, *72*, 217–266.
[14] A. Sachse, V. Hulea, K. L. Kostov, N. Marcotte, M. Y. Boltoeva, E. Belamie, B. Alonso, *Chem. Commun.* **2012**, *48*, 10648–10650.
[15] V. Smeets, C. Boissière, C. Sanchez, E. M. Gaigneaux, E. Peeters, B. F. Sels, M. Dusselier, D. P. Debecker, *Chem. Mater.* **2019**, DOI 10.1021/acs.chemmater.8b04843.
[16] V. Lafond, P. H. Mutin, A. Vioux, *Chem. Mater.* **2004**, *16*, 5380–5386.
[17] V. Smeets, L. Ben Mustapha, J. Schnee, E. M. Gaigneaux, D. P. Debecker, *Mol. Catal.* **2018**, *452*, 123–128.
[18] D. P. Debecker, P. H. Mutin, *Chem. Soc. Rev.* **2012**, *41*, 3624–3650.
[19] D. P. Debecker, C. Boissière, G. Laurent, S. Huet, P. Eliaers, C. Sanchez, R. Backov, *Chem. Commun.* **2015**, *51*, 14018–14021.
[20] J. T. Jankowiak, M. A. Barteau, *J. Catal.* **2005**, *236*, 366–378.
[21] W. Yuan, P. Yuan, D. Liu, W. Yu, M. Laipan, L. Deng, F. Chen, *J. Colloid Interface Sci.* **2016**, *462*, 191–199.
[22] S.-H. Kim, C.-K. Shin, C.-H. Ahn, G.-J. Kim, *J. Porous Mater.* **2006**, *13*, 201–205.
[23] X. Liu, C. Yang, Y. Wang, Y. Guo, Y. Guo, G. Lu, *Chem. Eng. J.* **2014**, *243*, 192–196.
[24] S. Flaig, J. Akbarzadeh, P. Dolcet, S. Gross, H. Peterlik, N. Hüsing, *Chem. Eur. J.* **2014**, *20*, 17409–17419.
[25] W. J. Kim, T. J. Kim, W. S. Ahn, Y. J. Lee, K. B. Yoon, *Catal. Lett.* **2003**, *91*, 123–127.
[26] F. Carn, A. Colin, M.-F. Achard, H. Deleuze, E. Sellier, M. Birot, R. Backov, *J. Mater. Chem.* **2004**, *14*, 1370–1376.
[27] P. Gaikwad, N. Bachelard, P. Sebbah, R. Backov, R. A. L. Vallée, *Adv. Optical Mater.* **2015**, *3*, 1640–1651.
[28] J. Wegner, S. Ceylan, A. Kirschning, *Chem. Commun.* **2011**, *47*, 4583–4592.
[29] L. van den Biggelaar, P. Soumillion, D. P. Debecker, *Catalysts* **2017**, *7*, 54.
[30] D. Pirozzi, M. Abagnale, L. Minieri, P. Pernice, A. Aronne, *Chem. Eng. J.* **2016**, *306*, 1010–1016.
[31] N. Brun, A. Babeau Garcia, H. Deleuze, M.-F. Achard, C. Sanchez, F. Durand, V. Oestreicher, R. Backov, *Chem. Mater.* **2010**, *22*, 4555–4562.
[32] A. Roucher, E. Roussarie, R. M. Gauvin, J. Rouhana, S. Gounel, C. Stines-Chaumeil, N. Mano, R. Backov, *Enzyme Microbial Technol.* **2019**, *120*, 77–83.
[33] D. P. Debecker, V. Hulea, P. H. Mutin, *Appl. Catal. A: General* **2013**, *451*, 192–206.
[34] S. Ungureanu, G. Laurent, H. Deleuze, O. Babot, M. F. Achard, M. I. Popa, C. Sanchez, R. Backov, *Colloids Surf. A* **2010**, *360*, 85–93.
[35] A. Thangaraj, M. J. Eapen, S. Sivasanker, P. Ratnasamy, *Zeolites* **1992**, *12*, 943–950.
[36] B. M. Reddy, B. Chowdhury, P. G. Smirniotis, *Appl. Catal. A: General* **2001**, *211*, 19–30.
[37] B. Erdem, R. A. Hunsicker, G. W. Simmons, E. D. Sudol, V. L. Dimonie, M. S. El-Aasser, *Langmuir* **2001**, *17*, 2664–2669.
[38] R. De Clercq, M. Dusselier, C. Poleunis, D. P. Debecker, L. Giebeler, S. Oswald, E. Makshina, B. F. Sels, *ACS Catal.* **2018**, 8130–8139.
[39] F. Chiker, F. Launay, J. P. Nogier, J. L. Bonardet, *Green Chem.* **2003**, *5*, 318–322.
[40] W. Panyaburapa, T. Nanok, J. Limtrakul, *J. Phys. Chem. C* **2007**, *111*, 3433–3441.

Self-standing titanosilicate monolith foams present hierarchical porosity, high Ti dispersion, and reach high TOF in the epoxidation of cyclohexene. A flow mode olefin epoxidation process is demonstrated.



*Valentin Smeets, Ludivine van den Biggelaar, Tarek Barakat, Eric M. Gaigneaux, Damien P. Debecker**

Page No. – Page No.

Macrocellular titanosilicate monoliths as highly efficient structured epoxidation catalysts

Macrocellular titanosilicate monoliths as highly efficient structured olefin epoxidation catalysts

Valentin Smeets,[a] Ludivine van den Biggelaar,[a] Tarek Barakat,[b] Eric M. Gaigneaux,[a] Damien P. Debecker[a,*]

[a] Institute of Condensed Matter and Nanosciences (IMCN), UCLouvain, Place Louis Pasteur, 1, Box L4.01.09, 1348 Louvain-la-Neuve, Belgium.

[b] Laboratory of Inorganic Materials Chemistry, UNamur, Rue de Bruxelles 61, 5000 Namur, Belgium

*E-mail : damien.debecker@uclouvain.be Tel. : +32 10473648.

Supplementary information

Materials

Preparation of the Si(HIPE) monolith foams[1]

6 g of HCl 37% wt. aq. (VWR) was added to 16 g of a freshly prepared solution of tetradecyltrimethylammonium bromide (TTAB, Acros Organics, 99%) 35% wt. aq. under stirring. Then, 5 g of tetraethyl orthosilicate (TEOS, Sigma-Aldrich, 98%) was added and the resulting clear solution was stirred for a few minutes at room temperature. The solution was then transferred into a crucible and 35 g of dodecane (TCI, > 99%) was added dropwise under continuous agitation, until a stable emulsion was formed. The latest was transferred in closed polypropylene flasks and allowed to rest for one week at room temperature. The monoliths were washed three times with 200 ml of acetone/tetrahydrofuran mixture (50:50, v/v) and then slowly dried at room temperature in a dessicator for 2–3 days. The dried material was calcined at 200°C for 2h (2°C/min) and then at 650°C for 6h (2°C/min) to remove the surfactant.

Preparation of the SiTi(HIPE) monolith foams

SiTi(HIPE)_1.8%. 6 g of HCl 37% wt. aq. and 0.125 g of titanium isopropoxide (TiiP, Acros Organics, ≥ 98%) were successively added to 16 g of a freshly prepared solution of TTAB 35% wt. aq. under stirring. The resulting clear orange solution was stirred for 1h at room temperature. After that time, 4.909 g of TEOS was added and the resulting solution was stirred for 2 min. The solution was then transferred into a crucible and 35 g of dodecane was added dropwise under continuous agitation, until a stable yellowish emulsion was obtained. The latest was transferred in closed polypropylene flasks and allowed to rest for one week at room temperature. The monoliths were washed three times with 200 ml of acetone/tetrahydrofuran mixture (50:50, v/v) and then slowly dried at room temperature in a dessicator for 2–3 days. The dried material was calcined at 200°C for 2h (2°C/min) and then at 650°C for 6h (2°C/min) to remove the surfactant.
SiTi(HIPE)_5%. The gel was prepared by the same procedure using 0.341 g of TiiP and 4.749 g of TEOS. Other quantities remained unchanged.
SiTi(HIPE)_10%. The gel was prepared by the same procedure using 0.682 g of TiiP and 4.499 g of TEOS. Other quantities remained unchanged.

Preparation of titanosilicalite-1 (TS-1)

The reference catalyst **TS-1** was prepared with a Ti loading of 1.8% (mol Ti / (mol Ti + mol Si) × 100 %) by hydrothermal synthesis according to a procedure from the literature.[2]

Characterization of the materials

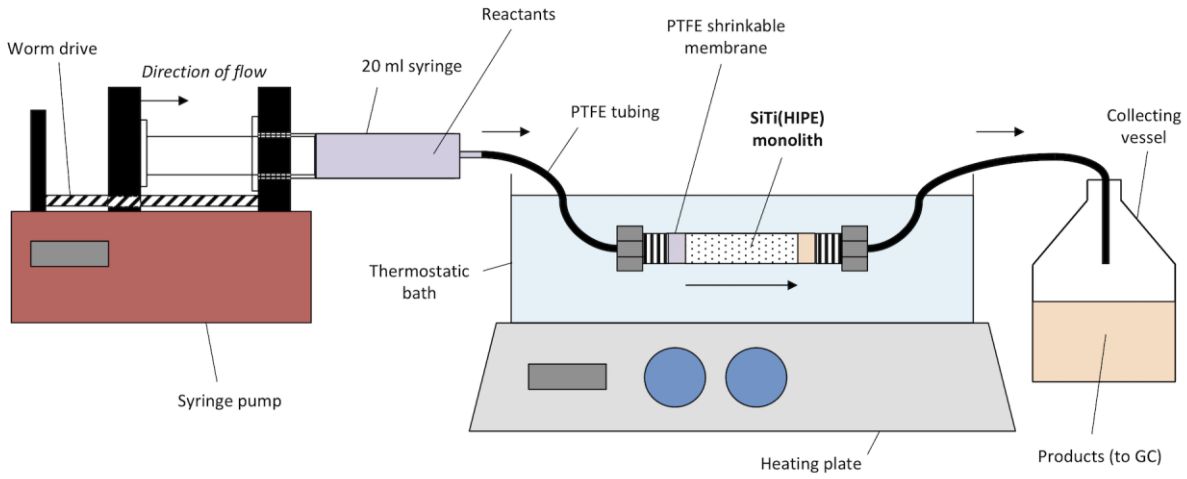
The Ti content of the materials was measured by ICP-AES on an ICP 6500 instrument (Thermo Scientific Instrument) after dissolution of the samples by sodium peroxide fusion. XPS experiments were carried out using an SSX 100/206 spectrometer (Surface Science Instruments, USA) with Al-Kα radiation operated at 10 kV and 20 mA. The binding energy scale was calibrated on the Si 2p peak, fixed at 103.5 eV.[3] The quantification of Ti in Ti–O–Si and Ti–O–Ti was based on the deconvolution of the $2p_{3/2}$ peak at approximately 460.0 and 458.5 eV, respectively.[4,5] Si was quantified on the basis of the Si 2p peak at 103.5 eV. The band gap energy (E_g) values were calculated from the optical absorption edge on DR UV-VIS spectra recorded on a Shimadzu UV-3600 Plus UV–Vis–NIR Spectrophotometer with a Harrick single-beam Praying Mantis Diffuse Reflectance collection system. The spectra were recorded at room temperature in 20000–50000 cm^{-1} range. A Spectralon® Diffuse Reflectance Standard was used to measure the background spectra. The DR UV-VIS spectra were background corrected and the Kulbelka Munk function was used to display the data. Scanning electron microscopy (SEM) images were taken

using a JEOL 7600F microscope at 15 kV voltage. Samples were pre-treated with a chromium sputter coating of 15 nm carried out under vacuum with a Sputter Metal 208 HR (Cressington). Textural properties were determined from N_2 adsorption/desorption isotherms at -196°C using a Tristar 3000 instrument (Micromeritics, USA). Prior to measurement, the samples were first degassed overnight under vacuum at 150°C. The surface area was evaluated by the BET method in the relative pressure range of 0.01–0.15 for the SiTi(HIPE) catalysts and of 0.01–0.05 for **TS-1**, in order to take into account the presence of micropores.[6] The micropore area and volume were evaluated by the t-plot method in the thickness range of 3.5–5.0 Å. The crush strength of the monoliths was deduced from the maximal compressive stress applied to the material at failure. The compressive stress was applied using a Mecmesin Advanced Force Gauge AFG 250N. The crush strength was obtained by reporting the compressive stress by the cross-section area of the monoliths. Mercury porosimetry measurements were carried out on a Micromeritics Autopore IV apparatus. The intrusion/extrusion isotherms were blank corrected using the same penetrometer connected to the same instrument port.

Catalytic procedures

The catalytic properties were investigated for the epoxidation of cyclohexene with cumene hydroperoxide as the oxidizing agent. The reaction in batch mode was carried out in a two-necked glass round-bottomed reactor at 90°C, equipped with a condenser, a magnetic stirrer and a rubber septum. In a typical run, 0.747 g (0.9 $mol.l^{-1}$) of cyclohexene (Sigma-Aldrich, 99%), 0.065 g (0.05 $mol.l^{-1}$) of nonane (TCI, > 98%) – used as the internal standard – and 50 mg (5 $g.l^{-1}$) of the catalyst were pre-mixed in 7.487 g of water saturated toluene (*ca.* 330 ppm H_2O) under stirring. After 10 min, 0.342 g (0.18 $mol.l^{-1}$) of cumene hydroperoxide (Sigma, 80%) was added and the mixture (10 ml total volume) was allowed to react for 3 h. The product formation was followed by collecting aliquots at regular time intervals and by analysing them in gas chromatography, using a Varian CP-3800 chromatograph equipped with a FID detector and a capillary column (BR-5, 30 m, 0.32 mm i.d., 1.0 μm film thickness). SiTi(HIPE) monoliths were ground into fine powder prior to measurement.

Continuous flow epoxidation was carried out using SiTi(HIPE) monolith casted in an inert heat-shrinkable polytetrafluoroethylene (PTFE) membrane connected to a syringe pump (ProSense) via PTFE tubing (**Scheme S1**)[1] The reactor was sealed by gently heating the membrane. After cooling down, the system was tested for leaks by immerging the reactor in a water bath and injecting air at the inlet. It was then immersed in an oil bath set at 90°C. The reactor was fed with a 20 ml reaction medium (same composition as in batch mode) kept in a syringe (HSW Norm-Ject). The flow rate was first set at 8.4 $\mu l.min^{-1}$ using the syringe pump and the reactor was conditioned for 24 h prior to the first measurement. The product quantification by gas chromatography was the same as described above.



Scheme S1. Experimental set-up used for the continuous flow epoxidation of cyclohexene using SiTi(HIPE) monolith.

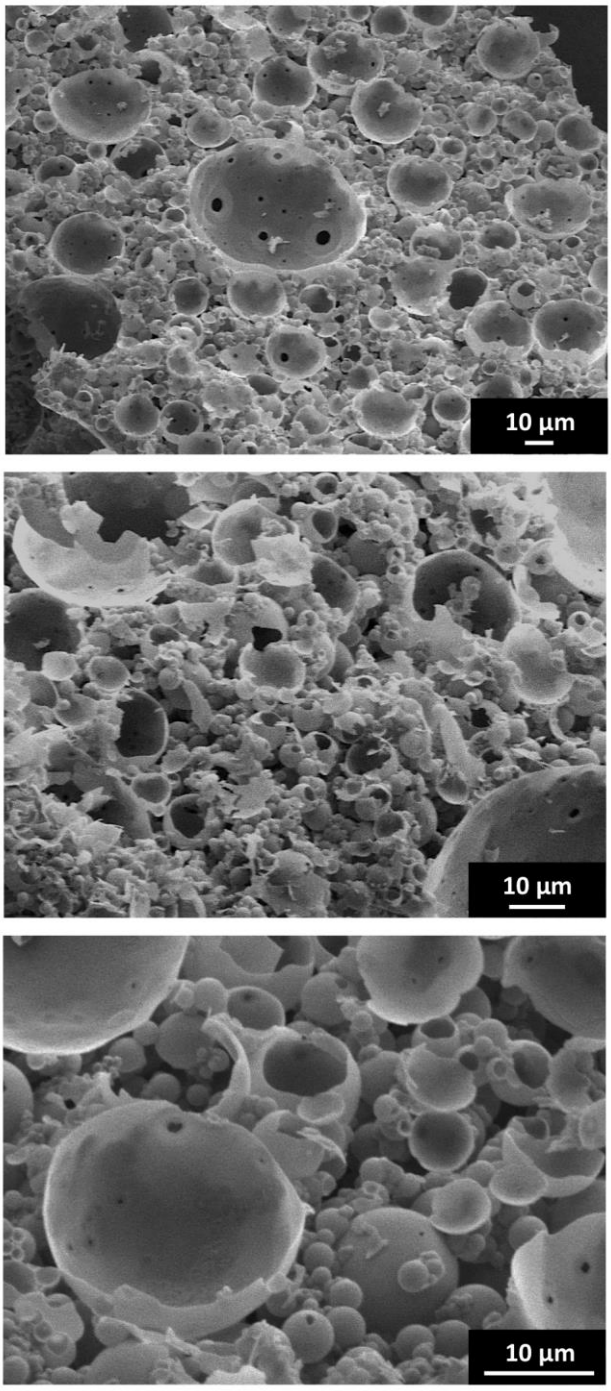


Figure S1. Additional SEM micrographs of **SiTi(HIPE)_5%**.

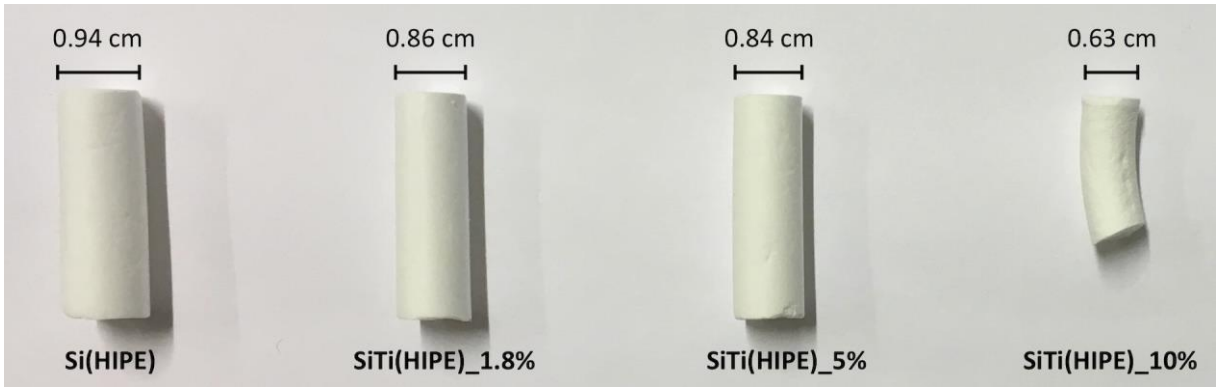


Figure S2. Additional pictures of the SiTi(HIPE) monoliths showing a macroscopic shrinkage due to the incorporation of increasing amount of titanium.

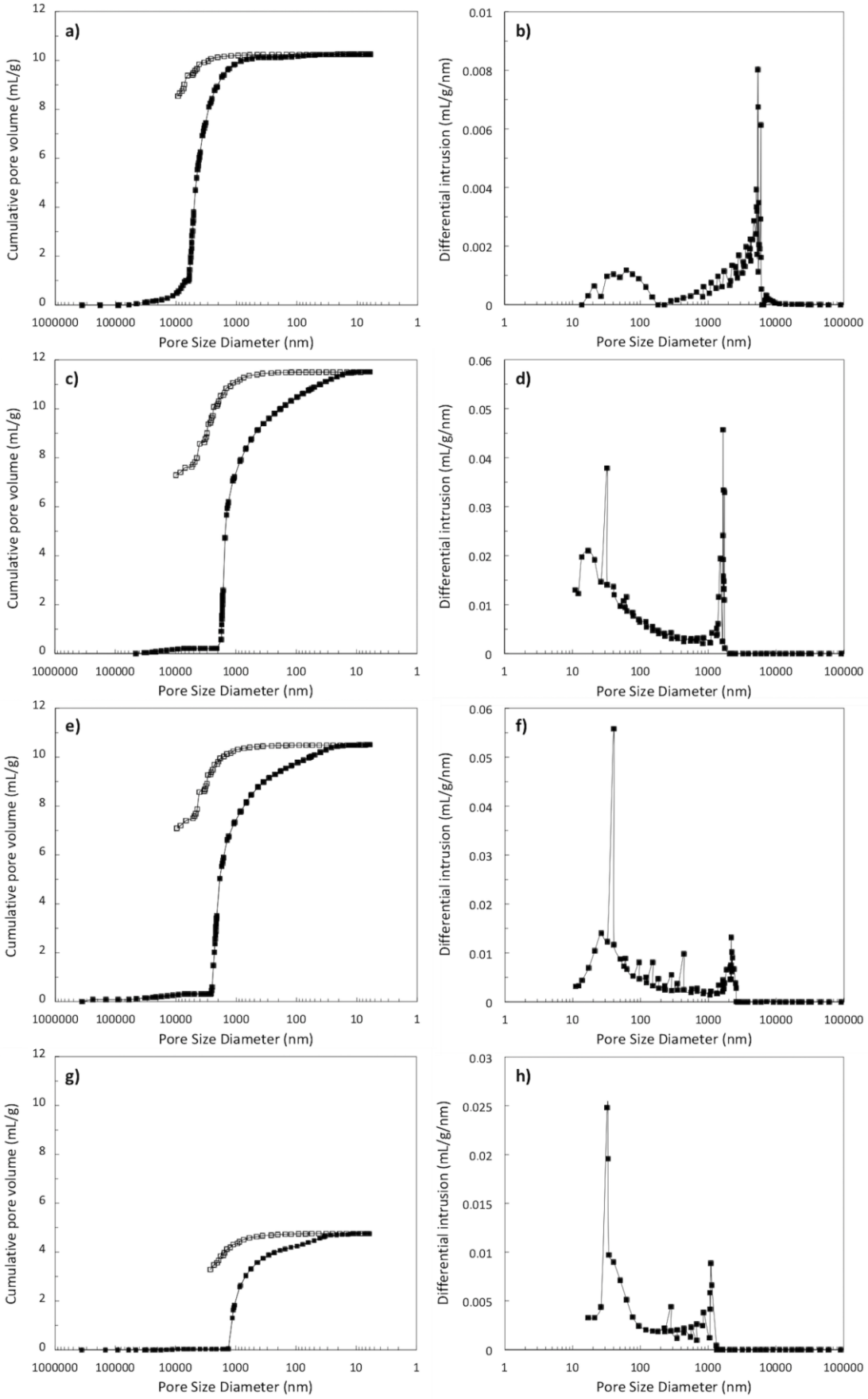


Figure S3. Mercury porosimetry intrusion-extrusion isotherms and pore size distributions (PSD) based on the intrusion data. a-b) **Si(HIPE)**, c-d) **SiTi(HIPE)_1.8%**, e-f) **SiTi(HIPE)_5%**, g-h) **SiTi(HIPE)_10%**.

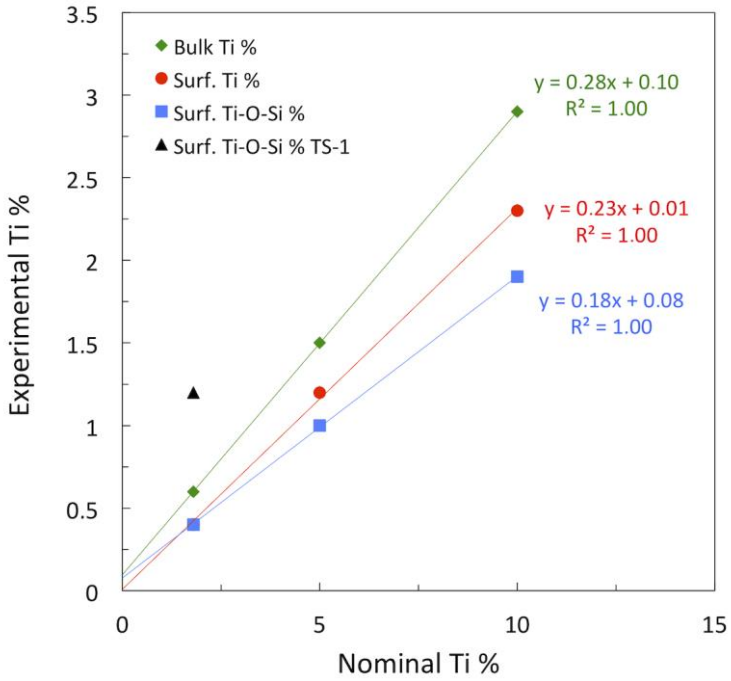


Figure S4. Correlations between the experimental and nominal Ti loading in the bulk (from ICP-AES) and at the surface (from XPS).

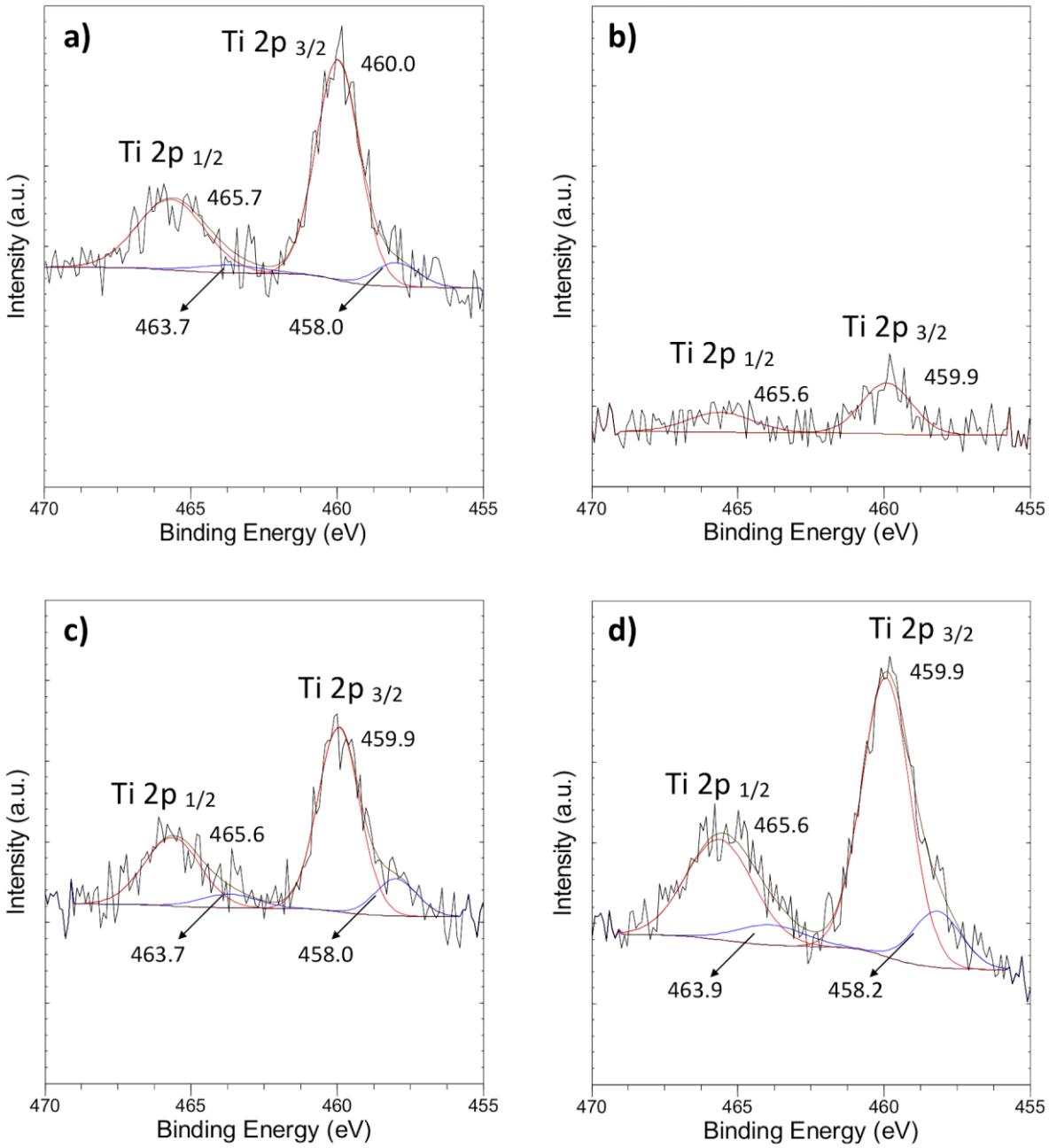


Figure S5. Deconvolution of the XPS Ti 2p spectrum of a) **TS-1**, b) **SiTi(HIPE)_1.8%**, c) **SiTi(HIPE)_5%** and d) **SiTi(HIPE)_10%**.

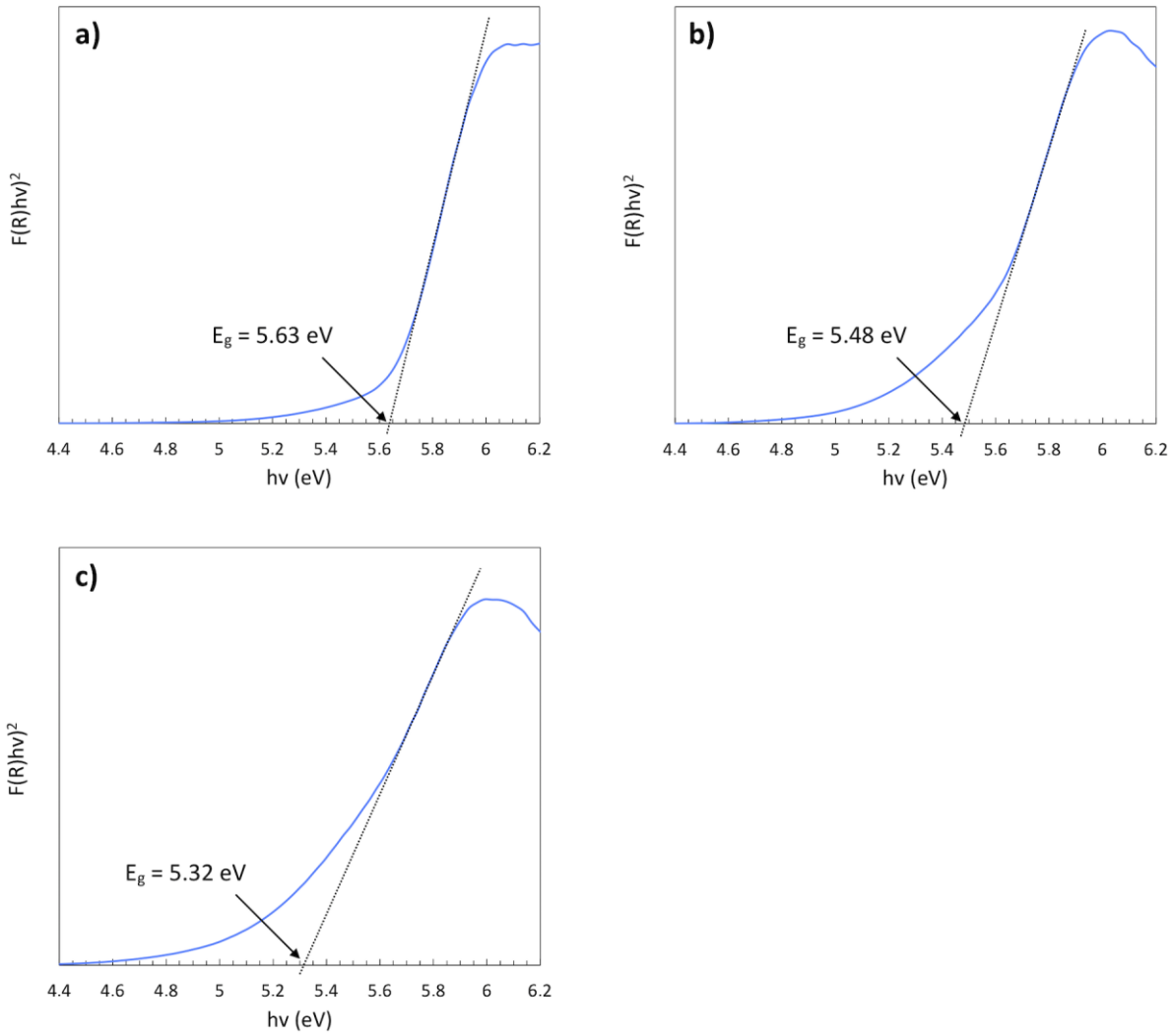


Figure S6. Estimation of E_g for a) **SiTi(HIPE)_1.8%**, b) **SiTi(HIPE)_5%** and c) **SiTi(HIPE)_10%** from the optical absorption edges. F(R) is the Kubelka-Munk function (normalized) and hν the incident photon energy.[7]

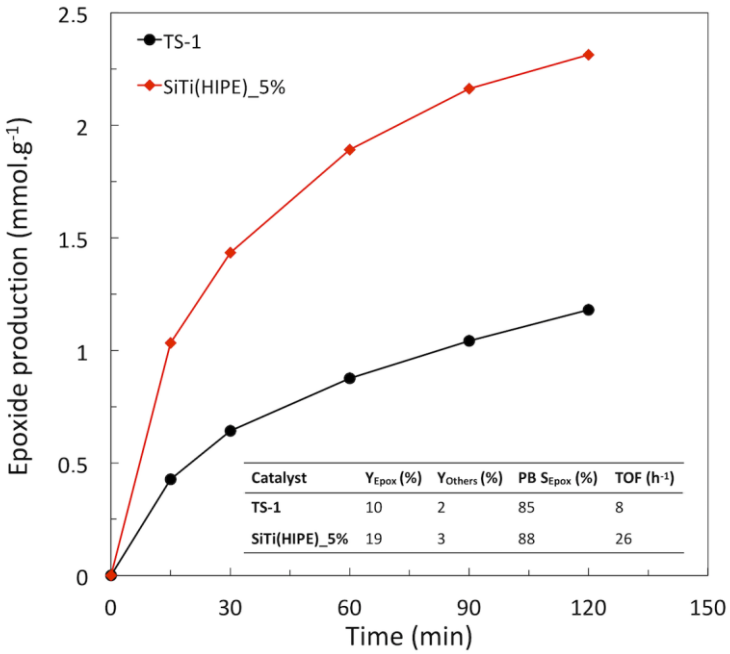


Figure S7. Cumulative epoxide production per gram of catalyst for the conversion of cyclohexene in acetonitrile with hydrogen peroxide as oxidant. The table in inset of the figure shows the corresponding yields (Y), selectivity (S) and initial turnover frequency (TOF). Each yield is defined as the ratio "amount of product" to "amount of H_2O_2 introduced", with "Epox" = cyclohexene oxide and "Others" = cyclohexane diol, 2-cyclohexen-1-ol and 2-cyclohexen-1-one. The product based selectivity toward the epoxide "PB S_{Epox}" is calculated by dividing the epoxide yield by the overall yield. The initial TOF is approximated from the overall yield at 15 min reaction time. It is defined as the number of mole of overall products formed per minute divided by the number of active sites (deduced from "Surf. Ti–O–Si %", **Table 2**). Experimental conditions: T = 60°C, [CATA] = 5 $g.l^{-1}$, [Cyclohexene] = 0.3 $mol.l^{-1}$, [H_2O_2] = 0.06 $mol.l^{-1}$.

Discussion: The results show a higher activity for the SiTi(HIPE) catalyst compared to **TS-1**, either in terms of yield (~2 times higher) or in terms of TOF, as the latter is of 26 h^{-1} for **SiTi(HIPE)_5%** and only of 8 h^{-1} for TS-1. With **SiTi(HIPE)_5%**, the selectivity for cyclohexene oxide reached 88% (vs. 85% for TS-1).

Test procedure: The catalytic tests in the presence of hydrogen peroxide were carried out in a two-necked glass round-bottomed reactor at 60°C, equipped with a condenser, a magnetic stirrer and a rubber septum. In a typical run, 0.249 g (0.3 $mol.l^{-1}$) of cyclohexene (Sigma-Aldrich, 99%), 0.046 g (0.05 $mol.l^{-1}$) of ^{toluene} (Sigma-Aldrich, 99.7%) – used as the internal standard – and 50 mg (5 $g.l^{-1}$) catalyst were pre-mixed in 7.500 g of acetonitrile under stirring. After 10 min, 0.068 g (0.06 $mol.l^{-1}$) of 30% (w/w) aqueous H_2O_2 (Sigma-Aldrich) was added and the mixture was allowed to react for 2 h.

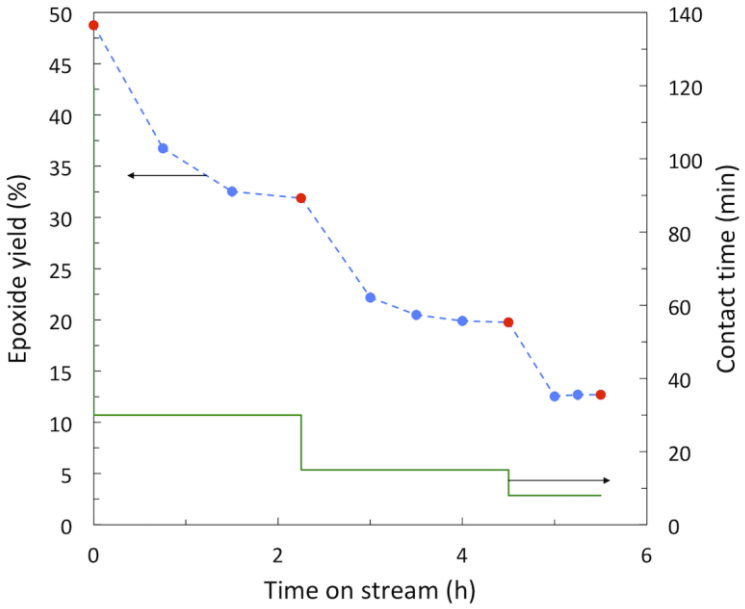


Figure S8. Epoxidation yield for the Ti-catalyzed conversion of cyclohexene with CHP using **SiTi(HIPE)_5%** in continuous flow mode. Red data points were plotted in Figure 5 as a function of the contact time.

Table S1. Results for cyclohexene epoxidation at 90°C (3h in batch reactor) with cumene hydroperoxide as oxidant

	Y_{Epox} (%)	Y_{Others} (%)[a]	X_{CHP} (%)	S_{Epox} (%)	Product based S_{Epox} (%)[b]	TOF (h^{-1})[c]
TS-1	20	3	16	126[d]	87	38
SiTi(HIPE)_1.8%	55	1	56	97	98	508
SiTi(HIPE)_5%	47	3	53	90	95	192
SiTi(HIPE)_10%	45	4	55	81	92	89

[a] Cyclohexane diol, 2-cyclohexen-1-one and 2-cyclohexen-1-ol

[b] These values have been calculated by dividing the epoxide yield by the overall yield instead of the CHP conversion

[c] The initial turnover frequency (TOF) value was approximated by the CHP conversion at 15 min reaction time. It is defined as the number of moles of CHP converted per minute divided by the number of active sites (deduced from "Surf. Ti–O–Si %", **Table 2**) one example of calculation is shown below.

[d] For **TS-1** catalyst, the selectivity value higher than 100% is associated with a CHP independent production of epoxide due to the role of molecular oxygen as initiator of a radical mechanism.

Example of calculation of the initial TOF calculated for **SiTi(HIPE)_1.8%** in the Ti-catalyzed cyclohexene epoxidation with cumene hydroperoxide (see **Table S1**):

$$\text{TOF} = \frac{\text{initial mol of CHP converted per minute}}{\text{number of active sites}} = \frac{0.0085\,\frac{60}{15}\,[\text{mol.g}_{\text{CATA}}^{-1}.\text{h}^{-1}]}{\frac{0.004}{0.996}\,[\text{mol Ti}^{4+}.\text{mol Si}^{-1}]\,\frac{1}{60.1}\,[\text{mol Si.g}_{\text{CATA}}^{-1}]} = 508$$

Where

$\frac{0.004}{0.996}$ mol Ti^{4+}. $molSi^{-1}$ is the number of moles of dispersed Ti divided by the number of moles of Si; this value is deduced from XPS results (see "Surf. Ti–O–Si %", **Table 2**)

And

$\frac{1}{60.1}$ mol Si. g_{CATA}^{-1} is the number of moles of Si per gram of catalyst; this value is calculated from the molecular weight of the mixed oxide $Si_{(1-x)}Ti_xO_2$, with x = 0.006 (see "Bulk Ti %, **Table 2**).

Table S2. Results for cyclohexene epoxidation at 90°C in continuous flow mode catalysed by **SiTi(HIPE)_5%**

Time on stream (h)	Contact time (min)	Y_{Epox} (%)	Y_{Others} (%)[a]	X_{CHP} (%)	S_{Epox} (%)	Product based S_{Epox} (%)[b]
0.00[c]	**120**	49	5	66	74	90
0.75	**30**	37	4	43	85	90
1.50		33	4	36	90	88
2.25		32	4	33	98	89
3.00	**15**	22	3	25	90	88
3.50		21	3	22	92	88
4.00		20	3	22	90	88
4.50		20	3	21	92	88
5.00	**8**	13	2	16	80	86
5.25		13	2	15	86	85
5.50		13	2	14	90	84

[a] Cyclohexane diol, 2-cyclohexen-1-one and 2-cyclohexen-1-ol
[b] These values have been calculated by dividing the epoxide yield by the overall yield instead of the CHP conversion
[c] This value has been measured after 24 h equilibration of the reactor with the reaction mixture at 8.4 $\mu l.min^{-1}$

References

[1] L. van den Biggelaar, P. Soumillion, D. P. Debecker, *Catalysts* **2017**, *7*, 54.
[2] A. Thangaraj, M. J. Eapen, S. Sivasanker, P. Ratnasamy, *Zeolites* **1992**, *12*, 943–950.
[3] M. Jacquemin, M. J. Genet, E. M. Gaigneaux, D. P. Debecker, *ChemPhysChem* **2013**, *14*, 3618–3626.
[4] B. Erdem, R. A. Hunsicker, G. W. Simmons, E. D. Sudol, V. L. Dimonie, M. S. El-Aasser, *Langmuir* **2001**, *17*, 2664–2669.
[5] B. M. Reddy, B. Chowdhury, P. G. Smirniotis, *Applied Catalysis A: General* **2001**, *211*, 19–30.
[6] J. Rouquerol, P. Llewellyn, F. Rouquerol, in *Studies in Surface Science and Catalysis* (Eds.: P.L. Llewellyn, F. Rodriquez-Reinoso, J. Rouqerol, N. Seaton), Elsevier, **2007**, pp. 49–56.
[7] R. De Clercq, M. Dusselier, C. Poleunis, D. P. Debecker, L. Giebeler, S. Oswald, E. Makshina, B. F. Sels, *ACS Catal.* **2018**, 8130–8139.